THE IMPACT OF OCEAN WAVES ON THE ATMOSPHERE

Peter A E M Janssen, James D. Doyle, Jean Bidlot, Bjorn Hansen, Lars Isaksen and Pedro Viterbo

ECMWF

Abstract

The air-sea momentum transfer is known to be affected by the state of the ocean waves. For example, young wind waves are usually steeper than old wind waves and therefore extract more momentum from the air flow. As a result airflow over young windsea is rougher than over old windsea. The sea state dependent momentum transfer is thought to be of importance in rapidly varying circumstances occurring near depressions and fronts and in fetch limited circumstances near coasts. In this paper we review previous results regarding the impact of ocean waves on the atmospheric climate and we discuss new results regarding the impact of waves on the atmosphere for medium-range weather forecasting. It is concluded that the impact of ocean waves on the atmosphere depends in a sensitive manner on the resolution of the atmospheric model (and to a lesser extent on the resolution of the wave model). In addition, analysis differences induced by the coupled wind-wave model increase the impact of ocean waves on the atmosphere by a factor of two. Overall, a modest positive impact on the scores of the atmospheric model is found while the improvements in the forecast performance of the wave model are even larger.

1. INTRODUCTION

Traditionally, many weather centres have applied their weather forecast to activities associated with the marine environment. Shipping, fisheries, offshore operations and coastal protection are, for example, all strongly dependent on weather and require marine weather forecasting extending to the limit of the medium- range forecasting period.

An important component of the marine weather forecast is the sea state. Wave forecasting using forecasted low-level winds started in the mid-sixties. Although, due to lack of knowledge of the basic processes governing wave evolution, the first ocean wave prediction models were certainly not perfect, it soon became evident that an important error source in forecast wave height was the wind speed error. This sensitive dependence of wave height results on the accuracy of the wind speed can be seen directly from the well- known empirical formula for the wave height in the special case of saturation under steady wind conditions. Denoting the significant wave height by H_S and the 10-metre wind speed by U_{10}, for saturated ocean waves we have the relation

$$H_S = \beta \frac{U_{10}^2}{g} \qquad (1)$$

where g is the acceleration of gravity and β a constant. Eq (1) follows from dimensional considerations and the assumption that the only relevant parameters in steady wind-generated, ocean gravity waves are g and U_{10}. Clearly, from (1) we infer that the relative error in wind sea wave height is twice the relative error in wind speed. It is therefore evident why ocean wave modellers have been critical regarding the quality of the generating wind field, often resulting in suggestions for improvement.

Ocean wave information can give benefits for atmospheric modelling and data assimilation. In particular, wave results have been used to diagnose planetary boundary problems, to obtain a consistent momentum balance at the ocean surface and to interpret satellite data. Firstly, this has resulted in an improved integration scheme for

vertical diffusion (*Janssen et al.*, 1992). Secondly, the momentum exchange between atmosphere and the ocean surface could be treated more accurately if the wave-induced drag were taken into account in a two-way interaction (*Janssen*, 1989); at present drag over the sea is modelled as a function of instantaneous wind speed only. Thirdly, the utilisation of satellite data from the scatterometer and Synthetic Aperture Radar (SAR) will benefit from both model generated and wave data for an optimal assimilation (*Stoffelen and Anderson*, 1995; *Hasselmann and Hasselmann*, 1991). Finally, because of the strong interaction between wind and waves, wave information may be beneficial for the atmospheric state when assimilated into a coupled ocean-wave, atmosphere model.

In this paper we concentrate on the two-way interaction of wind and waves and we study its consequences for both atmospheric and wave model results. In Section 2 we briefly describe the physics of air-sea interaction which includes the role of the wave-induced stress in the process of air-sea momentum transfer and we compare our model of the sea-state dependent roughness with in-situ data. Next, in Section 3 we discuss the impact of the modified momentum, heat and moisture exchange on a few synoptic cases, where in particular we study the role of resolution of the atmospheric and wave model. Furthermore, the impact of ocean waves on the atmospheric climate during the Northern Hemisphere winter, studied by Janssen and Viterbo(1996), is briefly reviewed. In Section 4 we describe our results for medium-range weather and wave forecasts. In these experiments both the analyses and forecasts were obtained with the coupled model and were compared with corresponding results from the uncoupled system. The analysis was performed with the three-dimensional variational approach (3DVAR), but we also will discuss one synoptic case obtained with the four-dimensional variational (4DVAR) assimilation scheme. We discuss differences in analysis and forecasts and considerable differences in surface pressure and wave height are found. Studying the scores we find a modest positive impact of two-way interaction on the atmospheric forecast model performance while there is larger improvement for wave height forecasts.

2. WIND WAVE INTERACTION

It has been known for some time that waves play an important role in the air-sea momentum transfer and it is of interest to address the consequences of the sea state dependence of the air-sea momentum transfer on the evolution of weather systems and on the atmospheric climate. During the last decade there has been considerable interest in the problem of the interaction of wind and ocean waves with emphasis on the sea state dependence of the momentum transfer across the air-sea interface. Experimental evidence has shown (see e.g. *Donelan*, 1982; *Smith et al.*, 1992) that, especially for young wind sea (as occurs e.g. near fronts or near the coast for offshore winds) the airflow depends on the sea state. Comparing young and old wind sea cases, the drag coefficient may vary by a factor of two. This suggests that the interaction process of wind and waves should be regarded as a two-way process. Parallel to this development a theory of two-way interaction of wind and waves was developed, giving the sea state dependence of momentum, heat and moisture transfer both for pure wind sea and mixed wind sea, swell cases (*Fabrikant*, 1976; *Janssen*, 1982, 1989, 1991; *Chalikov and Makin*, 1991). A parameterized version of the theory of momentum transfer is included in the latest cycle of the WAM model (*Komen et al.*, 1994).

Since the late 1950's (*Gelci et al.*, 1957) it is known that the basic evolution equation for ocean waves is the so-called energy balance equation for the two-dimensional wave spectrum. Although the general structure of the source functions of the transport equation was presented more than 30 years ago (*Hasselmann*, 1960) the early wave models did not attempt to compute the wave spectrum from first principles alone. The main reason was that the important role of nonlinear wave-wave interactions was not recognised. This changed by the 1970's when extensive wave growth experiments (*Mitsuyasu*, 1968, 1969; *Hasselmann et al.*, 1973) revealed the important role of the wave-wave interaction in controlling the shape of the wave spectrum. At that time a numerical implementation of the nonlinear interactions was computationally far too expensive, and thus wave modellers resorted to a simple parametrization which worked satisfactorily for locally-generated wind sea but

was known to have defects in mixed wind sea-swell situations. The weakness of this approach was most pronounced in the case of hurricanes because these have strong and rapidly-varying winds. As a result, a large international group of scientists (the so-called WAM = Wave Modelling Group) decided to develop a new wave model based on first principles, without relying on the somewhat artificial distinction between wind sea and swell.

The foundations of this new model were laid by Klaus and Susanne Hasselmann at the Max-Planck Institut für Meteorologie (Hamburg), where the deepwater version was developed. Since then many members of the WAM group have also contributed. For a complete account see *Komen et al.* (1994) where a thorough discussion on the energy balance equation, the physical foundations, the numerical aspects, verification of modelled results and assimilation of satellite data is given.

This newly developed model, called the WAM model, is based on the energy balance equation for the two-dimensional wave (surface variance) spectrum $F(f,\theta;\vec{x},t)$, which is a function of wave frequency f, direction θ, position $\vec{x}$ and time t,

$$\frac{\partial}{\partial t}F + \nabla \cdot (\vec{c}_g F) = S_{in} + S_{nl} + S_{ds}. \qquad (2)$$

.Here, $\vec{c}_g$ is the group velocity of the surface waves. The source functions S describe different physical processes: S_{in} represents the direct atmospheric input through the surface wind, S_{nl} represents resonant four wave interactions and S_{ds} is the dissipation term. Mean parameters such as wave height are derived as integrals of the wave spectrum. Operational running of the WAM model was not possible until recently, when an efficient algorithm for the computation of the nonlinear transfer became available (*Hasselmann et al.*, 1985) and when a reliable parametrization of the dissipation source function was found (*Komen et al.*, 1984). In addition, the determination of the surface stress (which is largely controlled by the wave-induced stress) was possible only after the work of *Janssen* (1989, 1991).

The WAM model does not impose any ad-hoc constraints on the spectral shape; the time evolution of the wave spectrum is computed by integrating the energy balance equation (2). In order to appreciate the role of the respective source terms, in Fig 1 we have plotted the WAM model's directionally averaged source functions S_{in}, S_{nl} and S_{diss} as function of frequency for young wind sea when a 20 m/s wind is blowing for just 3 hours. This Figure shows a typical picture of the energy balance for growing ocean waves, namely the intermediate frequencies receive energy from the airflow which is transported by the nonlinear interactions towards the low and high frequencies where it is dissipated by processes such as white capping. The consequence is that the wave spectrum shows a shift of the peak of the spectrum towards lower frequencies, while a considerable enhancement of the peak energy of the spectrum is also noticed in the early stages of wave growth. These results are in agreement with the findings from JONSWAP (*Hasselmann et al.*, 1973).

The latest version of the WAM model (WAM Cy4) has been operational at ECMWF since November 1991. The initial state for the wave forecast was constructed by forcing the WAM model with analysed ECMWF winds, and no wave data were used. Since August 1993 ERS-1 altimeter wave height data are assimilated by means of an Optimum Interpolation Scheme (*Lionello et al.*, 1992). In July 1994, spatial resolution was increased by a factor of two while in December 1996 spatial resolution was once more increased by a factor of three, so that the present operational model has effectively a resolution of 55 km. A summary of validation results over the year 1995 may be found in *Janssen et al.* (1997). This study has shown that the ECMWF wave forecasting system has reasonably good skill, but when wave forecasts are compared to their verifying analysis a significant, positive systematic error is found in the later stages of the forecast. This systematic error is in particular a problem in the Southern Hemisphere where it can amount to 10% of the mean wave height.

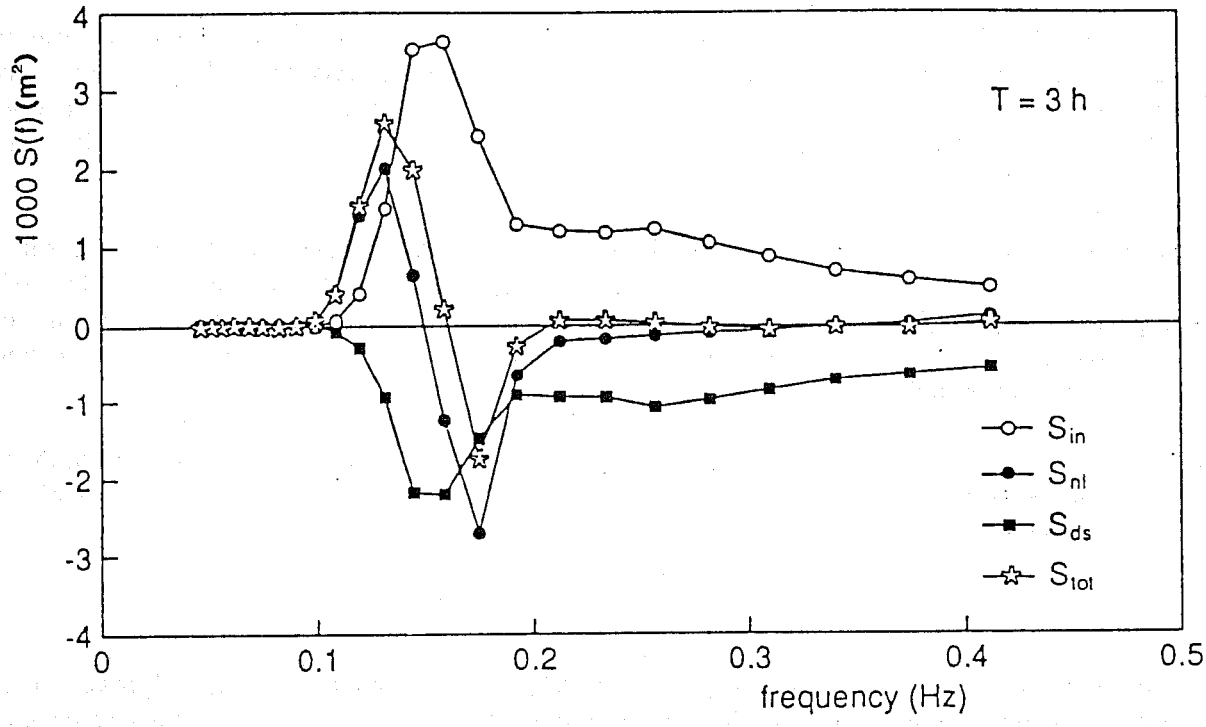

Fig. 1 Energy balance for young windsea.

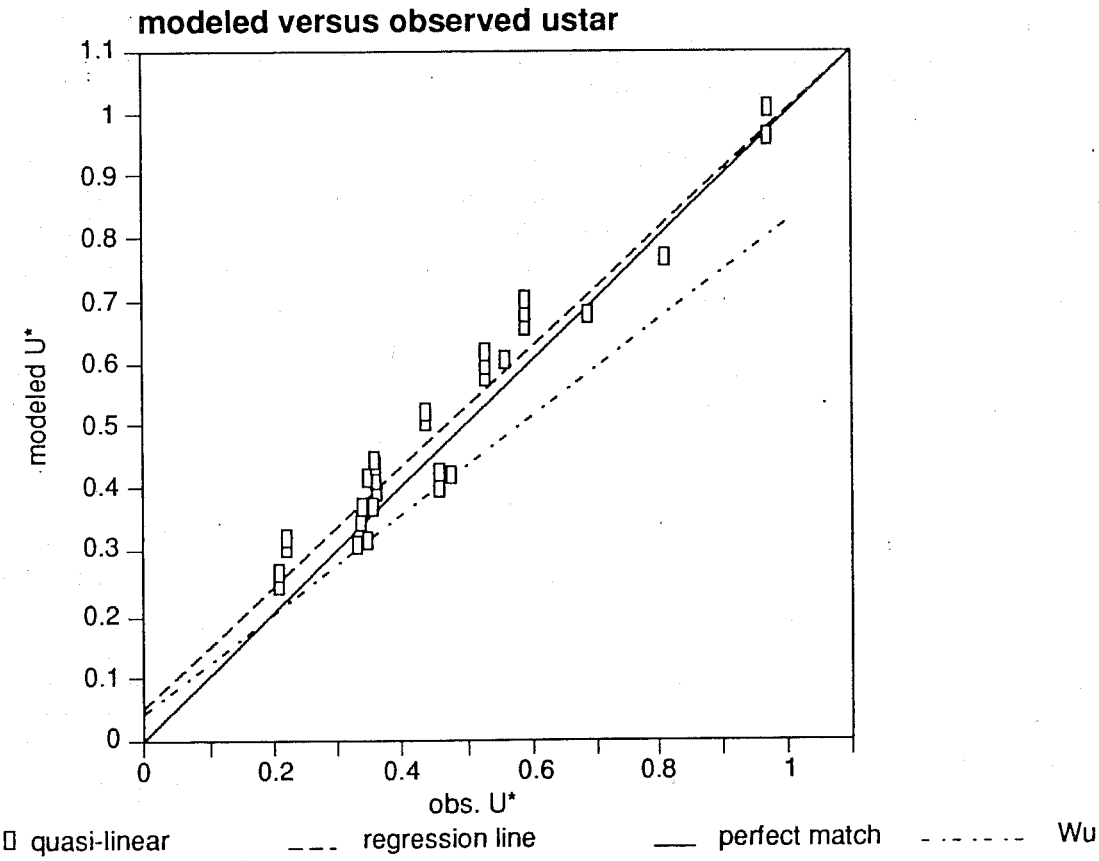

Fig 2 Comparison of modelled and observed friction velocity. The boxes indicate theory; the full line indicates a perfect match; and the dashed-dotted line indicates the Charnock relation according to Wu (1982).

In the ECMWF atmospheric model, the roughness length, z_0 of turbulent air flow over the ocean is presently parametrized by means of the well-known Charnock relation (*Charnock*, 1955)

$$z_o = \alpha u_*^2/g, \tag{3}$$

,where α is the Charnock parameter, g is the acceleration of gravity and u_* the friction velocity. As a result, the drag coefficient of the air flow increases with increasing wind speed. This is in sharp contrast to turbulent air flow over a smooth surface, where the drag coefficient decreases with increasing wind speed. Clearly, the difference in behaviour of the drag coefficient must be due to the momentum transfer to the ocean waves, including the unresolved short gravity waves. Prescribing these unresolved gravity waves by a Phillips spectrum (*Phillips*, 1958; *Banner*, 1990), the rate of change of wave momentum P due to wind is directly related to the so-called wave-induced stress τ_w, or

$$\tau_w = \int df d\theta \frac{\partial}{\partial t} P \tag{4}$$

where the wave momentum depends on the two-dimensional wave-variance spectrum $F(f,\theta)$ (which is determined by the energy balance (2)),

$$P = \rho_w g(f,\theta)/c \tag{5}$$

with c the phase speed ω/k of the waves, k is the wave number, ω is the angular frequency and ρw the water density. By means of the energy balance equation (2) one may write (4) as

$$\tau_w = \rho_w g \int df d\theta S_{in}/c \tag{6}$$

where S_{in} represents the wind input term which is proportional to the spectrum itself.The wave-induced stress is mainly determined by the high-frequency part of the wave spectrum because these are the waves that have the largest growth rate due to wind. Since it is known that the high-frequency part of the wave spectrum depends on the sea state (for example, young waves are steeper than old waves) it follows that the wave-induced stress depends on the sea state. Therefore, the Charnock 'constant' α should depend on the sea state as well. Based on the so-called quasi-linear theory of wind-wave generation (*Janssen*, 1982), which determines the slowing down of the wind because of the air-sea momentum transfer, *Janssen* (1991) found the following dependence of the Charnock parameter α on the wave-induced stress τ_w,

$$\alpha = \beta\left(1 - \frac{\tau_w}{\tau}\right)^{-1/2}, \beta = 0.01 \tag{7}$$

where $\tau = \rho_a u_*^2$. In the absence of surface gravity waves ($\tau_w = 0$), Eq (7) parametrizes the momentum loss due to processes which have not been considered so far, for example the growth of capillary waves or the interaction with currents, while in the presence of gravity waves ($\tau_w \neq 0$) the air flow becomes rougher because these waves also extract momentum from the air.

The validity of Eq (7) to determine the surface stress has been checked by *Janssen* (1992) using HEXOS data (*Smith et al.*, 1992). During HEXOS, the wind speed U_{10}, friction velocity u_* and the one-dimensional frequency spectrum were measured simultaneously. Using the wind input term S_{in} from the WAM model the wave-induced stress may therefore be determined and for known observed wind speed U_{10} the friction velocity u_* is obtained by solving

$$u_* = C_D^{1/2} U_{10} \qquad , C_D = \left(\frac{k}{(In10)/z_o}\right)^2 \tag{8}$$

iteratively. Here z_0 is given by (3) with Charnock parameter (7). The comparison of modelled and observed friction velocity is given in Fig 2 and the agreement is good.

The HEXOS data consisted of cases of relatively young wind sea. However, old wind sea cases are treated by Eq(6) equally well. This is shown in Fig 3 where, for the North Atlantic area, we present the relation between drag coefficient C_D and wind speed (both at height of 31 m) for a summer case in July 1992 and a winter case in January 1991. The drag coefficient according to the Charnock relation (with Charnock constant $\alpha = 0.0185$) is also given. The drag coefficients were obtained from the coupled WAM-ECMWF model, details of which will be given shortly. It is clear from Fig 3 that the relationship between drag coefficient and wind speed depends on the season; in summer this relation closely follows that of Charnock, while in winter large deviations from the Charnock relation may be noted, especially for storms with a strong curvature, where relatively young wind sea may occur.

From all this it may be concluded that, depending on the sea state, the drag coefficient may vary by a factor of two for the same surface wind speed. Therefore, one may wonder whether two-way interaction has impact on the evolution of an individual depression, on medium-range forecasting in general and on the mean atmospheric circulation.

In the following, impact of ocean waves on the atmospheric model will be studied by means of a coupled atmospheric, ocean wave model. The coupling scheme is a simple one: ocean waves are driven by atmospheric winds, while the sea-state dependent slowing down of these winds is parametrized by the Charnock parameter given in Eq (7).

3. IMPACT ON SYNOPTIC CASES AND ON CLIMATOLOGY

3.1 Impact on a single depression

The impact of two-way interaction on the evolution of a single depression was recently studied by *Doyle* (1994). The atmospheric model used in this study is the Navy's Coupled Ocean Atmospheric Mesoscale Prediction System (COAMPS) and the wave model is the WAM model coupled through Eq (7). The three-dimensional model solves the compressible equations of motion. The model is used in a channel mode with the f-plane approximation. In the vertical the model has 32 layers with greater resolution in the lower troposphere (13 layers below 850 mb) to enable a good representation of the interaction of the wave-induced stress with the marine boundary layer.

For both atmospheric and WAM model the horizontal resolution is 30 km while periodic conditions were applied in the zonal direction. A timestep of 90 s is used in the atmospheric model and 6 min. for the ocean wave model. The simulation is integrated to 96 h which enables the rapid development and early decay phases of the idealised cyclone to be studied.

The initial condition consists of a zonally symmetric jet stream based on mean winter conditions, where the initial temperature distribution is found from thermal wind balance. The initial moisture field is based on climatology as well. The initial perturbation of the baroclinically unstable jet was provided by a small longitudinal wind component below 250 mb, specified as a sinusoidal function that damps near the boundaries. The sea surface temperature pattern resembled the Gulf Stream pattern.

The sea level pressure at 60 hrs. for the control run (i.e. constant Charnock parameter = 0.0185) and the coupled run (i.e. two-way interaction) is presented in Fig 4. It clearly shows that, due to the increased roughness in the coupled run, the central pressure of the low is 6 mb higher compared to the control run. The time evolution of

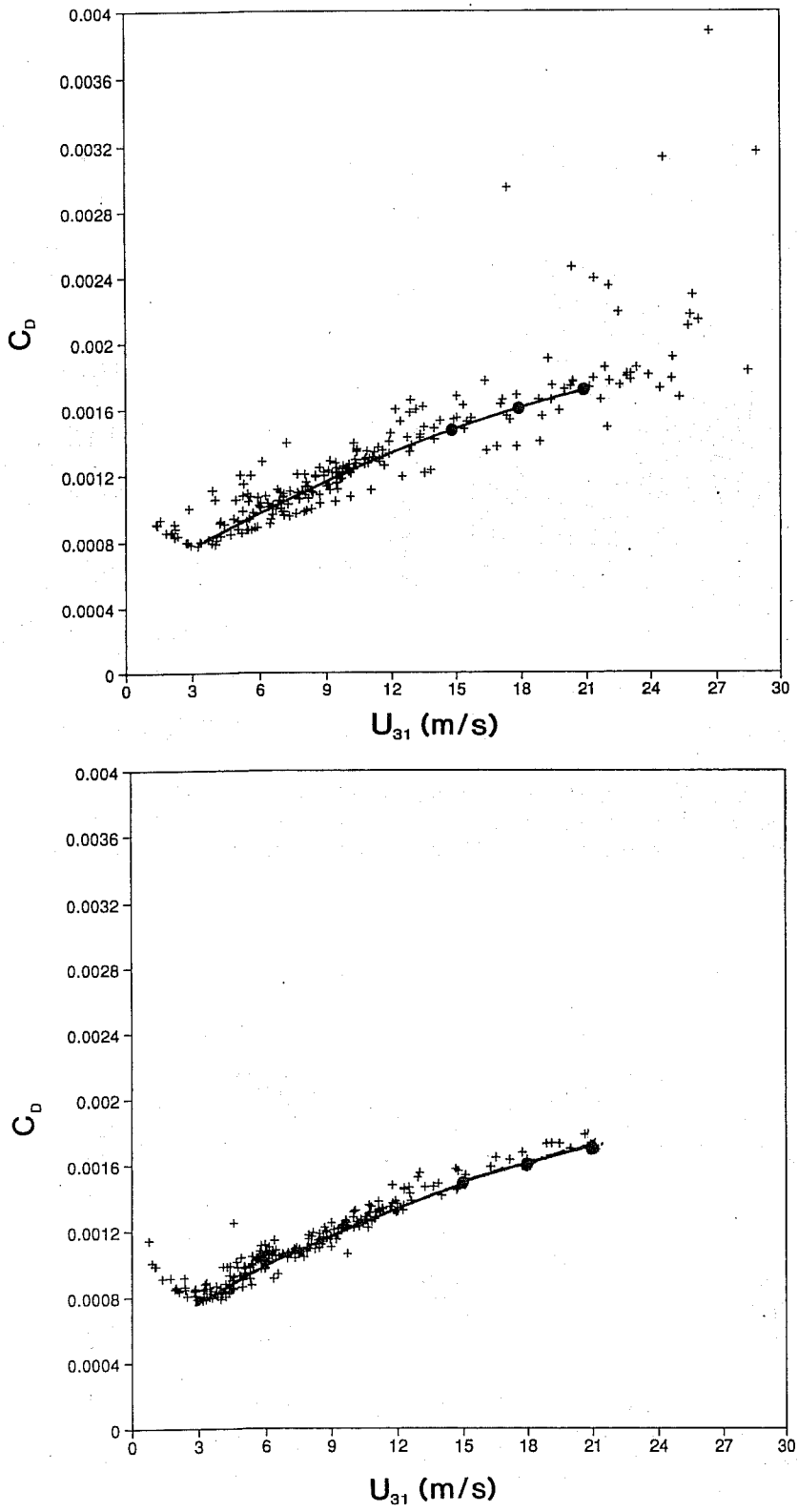

Fig 3 Drag coefficient versus lowest level wind for the North Atlantic area during a time in winter (top) and summer. The Charnock relation is shown as well.

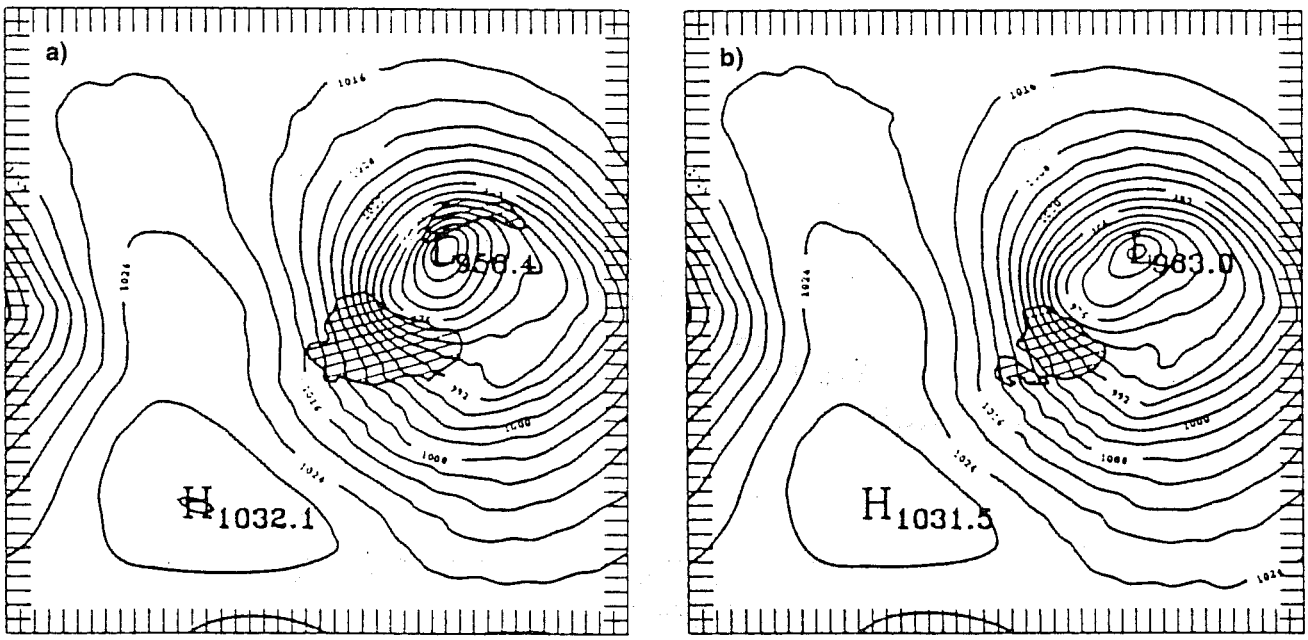

Fig 4 Simulated sea-level pressure for a) control and b) coupled simulations for the 60h time. The isopleth interval is 4 mb. Regions of lowest model layer wind speed in excess of 25 m/s are denoted by shading. Tick marks are plotted along the borders every third grid point or 90 km. (From Doyle, 1994, with permission.)

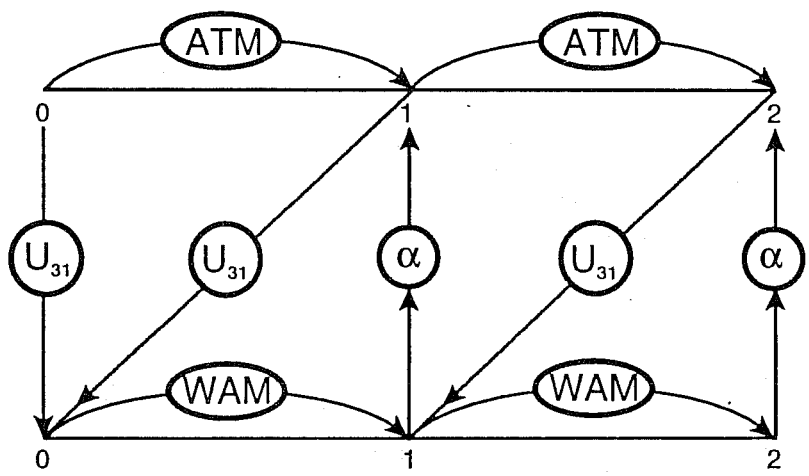

Fig 5 Schematic of the coupled system.

the central pressure (not shown) confirms this picture. The increased roughness in the coupled run is accompanied by an increase in sensible heat flux of about 20%, the rainfall maximum increases by 34%, while the kinetic energy at the surface decreases by 20%. These results indicate that frictional effects of wind-generated ocean waves may influence the boundary layer structure in the vicinity of a marine cyclone.

Doyle's results are encouraging and do suggest that in extreme conditions the sea state dependent roughness make a difference for the evolution of a low. However, in order to obtain impact a very high resolution atmosphere and wave model was used while time steps were very short, in the order of a few minutes. For operational, global weather forecasting these choices are not yet feasible and therefore it is of interest to study the impact of ocean waves on a state of the art operational weather prediction model.

A scheme to couple the WAM model and the ECMWF model was developed, which was similar in spirit to the one developed by *Weber et al.* (1993) and *Doyle* (1994) (see also *Janssen,1994)*. The atmospheric model is run for a number of time steps, then a wave forecast is run using the lowest level winds (U_{3l}) produced by the atmospheric model after which the atmospheric model is run for the next period, now using the Charnock parameter (α) as determined by the WAM model during the previous interaction period. A schematic view is given in Fig 5. In the present setup we have taken, following Beljaars (1995), neutral exchange coefficients for momentum, heat and moisture that differ from each other. This means that compared to momentum transfer, heat and moisture transfer have a reduced dependence on the sea state because they depend on the square root of the drag coefficient. The extended range integrations on which we report in Section 3.2 had identical exchange coefficients but we checked that this assumption had hardly any influence on the results.

In the remainder of this paper we shall discuss the impact of two-way interaction on the atmospheric circulation. We measure this impact by comparing results of two-way interaction with results of one-way interaction experiments. The one-way interaction experiments are performed with the same software as the two-way experiments except that in the one-way experiment, which will be called the control from now on, the Charnock parameter takes the constant value 0.018, while in the two-way experiment (coupled for short) the Charnock parameter is determined from the wave model, thus giving a consistent energy balance at the surface.

In order to distinguish between different versions of the coupled code we introduce the following notation: Txxx/Lyyy-z.zD denotes the coupling of an atmosphere model, having a triangular truncation of Txxx and yy Layers, with a wave model which has a resolution of z.z degrees. Most of the results discussed in this paper are obtained with the T213/L31-1.5D version of the coupled system while we also discuss some results from the T213/L31-0.5D version.

We have performed with the T213/L31-0.5D version of the coupled system an extensive set of 10 day forecasts on 'randomly' selected cases by choosing as initial conditions the 15th of every month in the period of September 1996 until August 1997. The control results were obtained with CY18R1 of the ECMWF atmospheric model.

The initial data for the atmospheric fields were taken from the analysis provided by the atmospheric model which was operational at the start of the forecast. The initial data of the WAM model were generated by using as initial condition a so-called JONSWAP spectrum 10 days before the starting date of the forecast and by running the wave model until the starting date of the experiment with analysed winds from the ECMWF archive.

Comparing scores of the anomaly correlation of 1000 and 500 mb height of the coupled and control runs we found hardly any differences, except over the North Pacific where the coupled run showed a small beneficial impact of ocean waves on the atmosphere (not shown). Nevertheless, occasionally considerable synoptic differences between the coupled and control run are found. An example is the 4 day forecast from the 15th of February 1997, shown in Fig.6. This low was observed during FASTEX and was called IOP 17.The left top

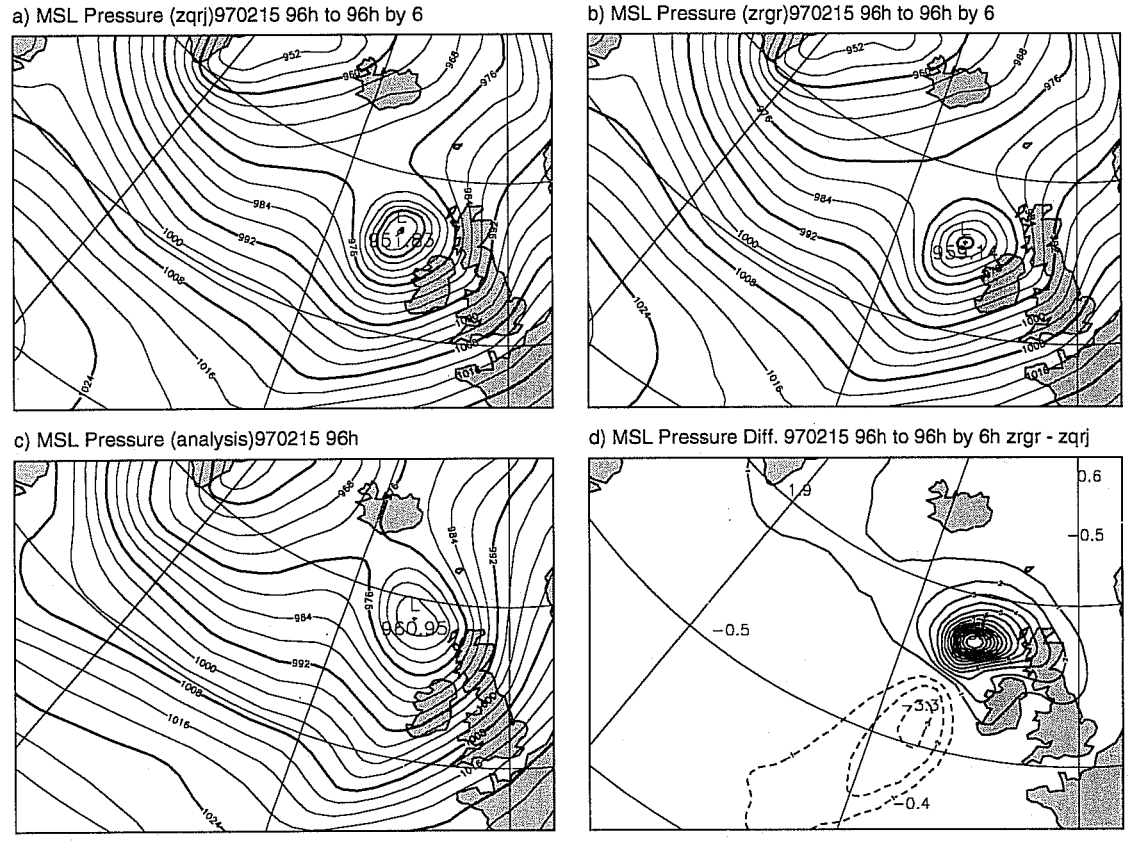

Fig 6 Comparison of 4-day forecast of surface pressure over the North Atlantic for the 15th of February 1997. Top left panel: Control. Top right panel: coipled. Bottom left panel: operational analysis. Bottom right panel: the difference between coupled and control. Version of coupled model is T213/L31-0.5D.

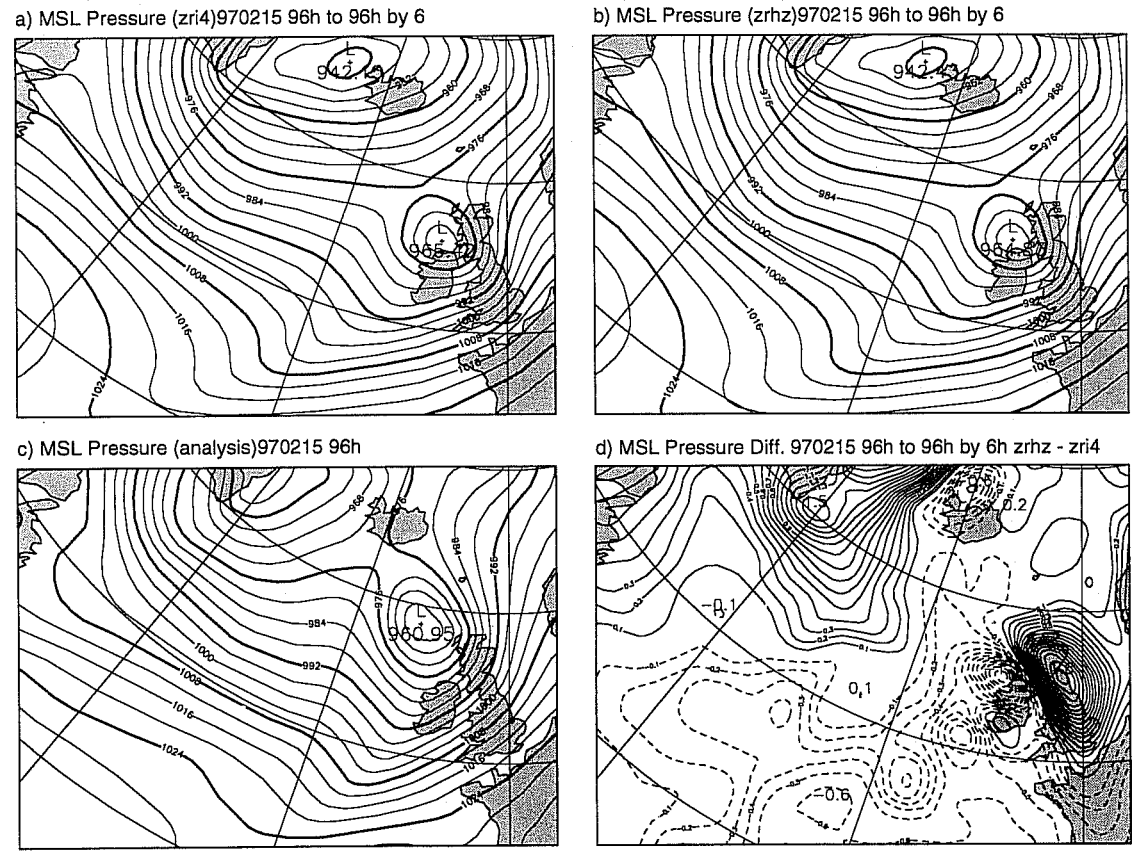

Fig 7 The same as fig. 6 but now for T106/L31-1.5D version.

panel of Fig. 6 shows the surface pressure over the North Atlantic for the control run, the top right panel shows the coupled results, the bottom left panel shows the operational verifying analysis, while the bottom right panel shows the difference between coupled and control. The control day 4 forecast has a good quality, as may be judged from the comparison with the analysis although the low near Greenland is too deep by 5 mb and the fast moving low west of Scotland is misplaced and too deep by about 9 mb. The anomaly correlation over the North Atlantic area was larger than 90%. In the coupled run it is seen that both lows are less deep (the one near Scotland even by 8 mb) so that in this respect there is better agreement between the coupled run and the verifying analysis. However, because the differences are small scale, there is hardly any difference in anomaly correlation between coupled and control run.

It is emphasized that these results depend in a sensitive manner on the resolution of the coupled system. To appreciate this point we show in Fig. 7 results of the T106/L31-1.5D model for the same case. While in the high resolution run we notice differences of up to 15 mb, the low resolution results show only differences of at most 2 mb. A similar sensitive dependence on resolution was also noticed in other extreme events. An example, not shown here, is the so-called Braer storm of the 11th of January 1993.

On average the time scale of impact of waves on the atmospheric circulation is about 5 days. This time scale of impact is related to the decay of vorticity by surface friction. Using the quasi-geostrophic approximation (*Pedlosky*, 1987) the rate of change of vorticity may be related to the curl of the surface stress, while the surface stress is related to the geostrophic wind by means of an empirical geostrophic drag law. As a result, the decay law due to surface friction for the large-scale vorticity ζ becomes

$$\frac{\partial}{\partial t}\zeta = -\gamma\zeta \qquad ,\gamma \approx \frac{C_{Dg}U}{D}$$

where U is the geostrophic wind speed, D is the equivalent depth and C_{Dg} the geostrophic drag coefficient,

$$C_{Dg} = \left(In\frac{\frac{k}{0.2u_*}}{fz_o} \right)^2$$

with f the coriolis parameter and k the von Karman constant. At this point it is important to argue why young wind sea is relevant at all for the evolution of a depression, since, as seen from the waves, the lifetime of young windsea is only 6-12 hours. However, for an observer moving with a depression the young windsea state may last several days or even longer, depending on its speed and curvature. For a geostrophic wind speed of 25 m/s and an equivalent depth of 5 km one finds for young wind sea (Charnock parameter $\alpha = 0.09$) a damping rate of 0.4 days^{-1} while, for old wind sea ($\alpha = 0.018$), a damping rate of 0.3 days-1 is found. Compared to growth rates of the baroclinic instability without surface friction (these are typically 0.6 days-1) it is seen that the damping rates due to surface friction must have a considerable impact on the overall growth rate of the vortex (depression). Different sea states may therefore give rise to differences in the total growth rate of about 25% so that significant differences only occur over a timescale of 5 days. Because of this long timescale it should be noted that this simple picture of the impact of surface friction on the decay of a depression may be obscured by nonlinear wave-wave interactions and wave-mean flow interaction. In addition, it should be realized that enhanced surface roughness not always will lead to a decay of the depression, because heat fluxes are enhanced as well which may result in vortex stretching and therefore in a deepening of the low. Thus, whether due to the enhanced roughness (as caused by the ocean waves) there is filling up or a deepening of a low depends on whether momentum or heat fluxes determine the evolution of that particular low.

3.2 Extended range forecasting

We have seen that two-way interaction may have impact on synoptic cases and the question of interest is whether there is any systematic impact of waves on the atmospheric circulation. Hence this requires a study with the coupled model over time scales of a season. To that end we performed a number of 120 day runs with the T63/L19-3.0D version of the coupled model and compared the mean over the last 90 days with results from the model with one-way interaction only. We concentrate here on the winter season of 1990. In order to obtain reliable information on the impact of waves on the atmospheric circulation there is a need for ensemble forecasting (see e.g. *Ferranti et al.*, 1993). The variability in the Northern Hemisphere is high, especially over the oceans. We therefore performed 15 coupled and control runs for the winter season of 1990 starting from the analysis of 15 consecutive days, thus providing a reliable estimate of the mean state of the atmosphere at a certain location. At the same time we may infer information on the variability from the scatter around the mean, thus a student t-test may be applied to test statistical significance of the mean difference between coupled and control run.

Results are discussed in detail by *Janssen and Viterbo* (1996). Here we only discuss features in the 500 hPa height field. In Fig 8 we have plotted the ensemble mean of 500 hPa height field and their differences for the Northern Hemisphere while, for comparison purposes, we also display the 90 day mean of the corresponding ECMWF analysis. Fig 9 shows a similar plot for the Southern Hemisphere. Contours in the mean 500 hPa height field are plotted every 60 m, while in the difference plot we have indicated by dark shading the probability of 95% (or more) that the two fields in question are not equal. Significant differences are noted in the storm track areas in both hemispheres. In the Northern Hemisphere we note differences over the Northern Pacific, Europe and Siberia. In the last two areas the coupled climate shows, when compared to the analysed climate, a considerable improvement. This is, however, unclear for the Northern Pacific. There are also differences in the low and high frequency variability (not shown). Over the North Atlantic a small shift in storm track is to be noted while the low frequency variability over Europe drops by 25%. The impact of waves in the Southern Hemisphere appears to be large scale; the storm track has, in the coupled climate, a more "wavy" character. East of New Zealand the coupled climate shows improvement when compared to the analysed climate. It is also of interest to show the ensemble mean of wave parameters. Fig 10 shows the mean wave height for coupled run, control run and the difference. Differences are of the order of 20-30 cm which is about 10% of the mean wave height; they are large-scale, especially in the Southern Hemisphere, with generally a reduction in wave height. For the Southern Hemisphere (between 20°S and 60oS) the mean bias between coupled and control runs is -20 cm. Although this is not sufficient to alleviate the systematic error problem noted in the 10 day forecast verification (Sections 2), it certainly works in the right direction. The reason for the lower wave height in the coupled run is a slowing down of the air flow. This is evident in Fig 11 where the mean friction velocity for coupled and control run and the difference is shown. In the Southern Hemisphere a shift in the storm track is evident, while also in the Northern Pacific some important changes are to be noted. Finally, in the tropics we see an increase of stress in the coupled model, especially in the warm pool area[1]. This change in the tropics may have important consequences for tropical ocean circulation modelling and hence for seasonal forecasting.

4. MEDIUM-RANGE FORECASTING

In this Section we discuss some results from experiments where both the analysis and forecasts are obtained with the coupled model and we compare with corresponding analyses and forecasts of the uncoupled system.

1. The reason for the increase of stress and wind speed in this area is not clear. It may be pointed out, however, that the wave field in the warm pool mainly consists of swell which has a small wave-induced stress, thus the Charnock constant is smaller than its value in the control run. This could give rise to higher winds.

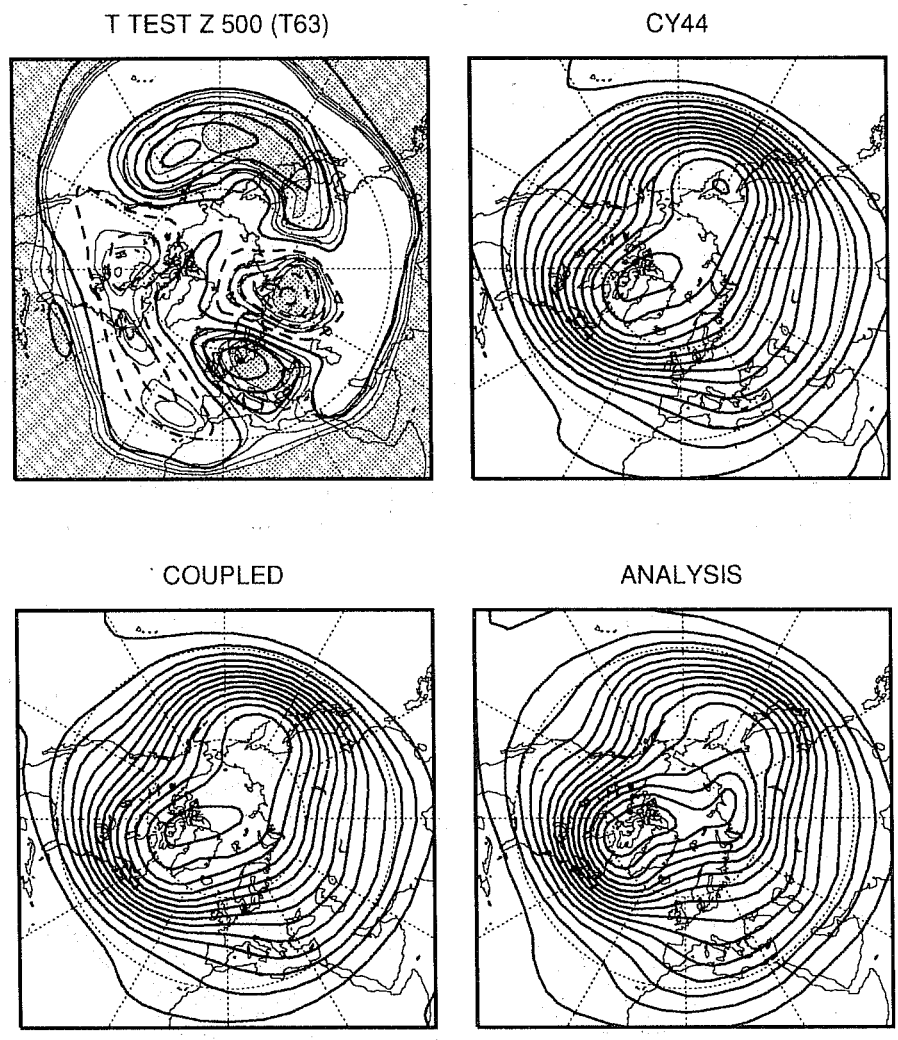

Fig 8 Ensemble mean of 500 mb geopotential height of coupled and control run and their differences. For comparison also the analysed climate is shown. Period is winter 1990 and area is Northern Hemisphere.

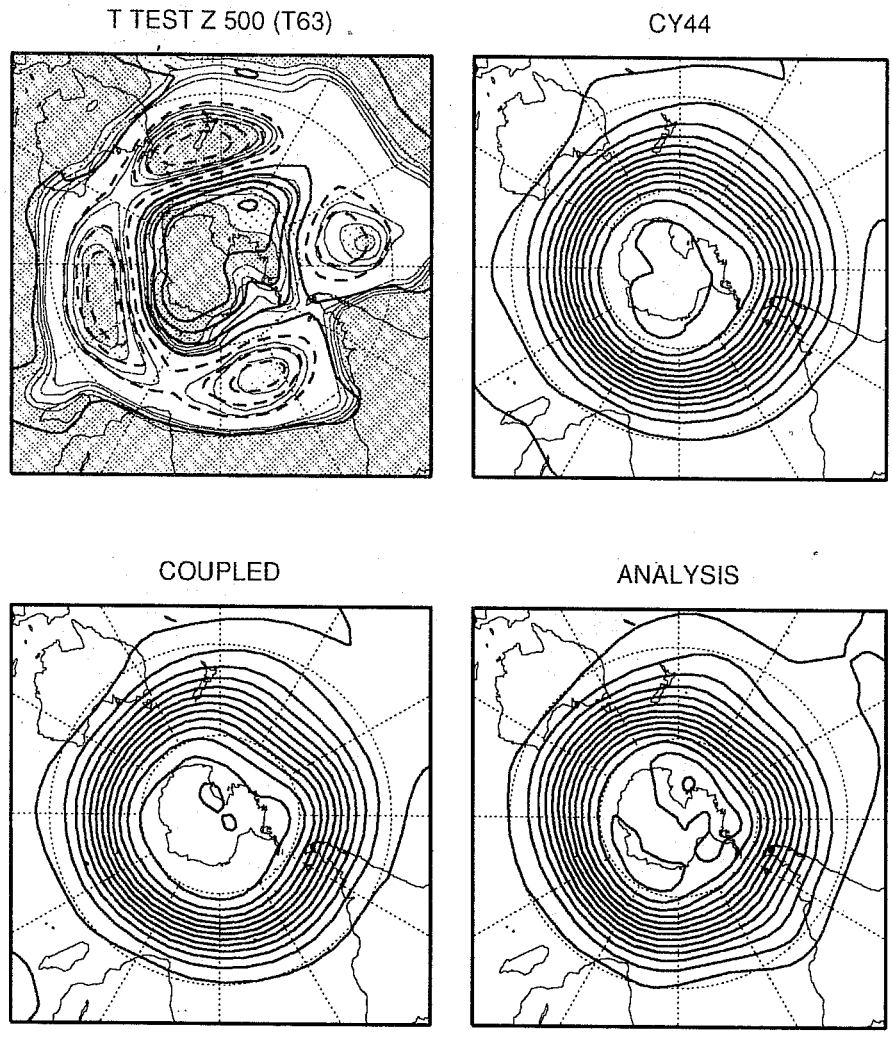

Fig 9 Same as Fig 8 but now for Southern Hemisphere.

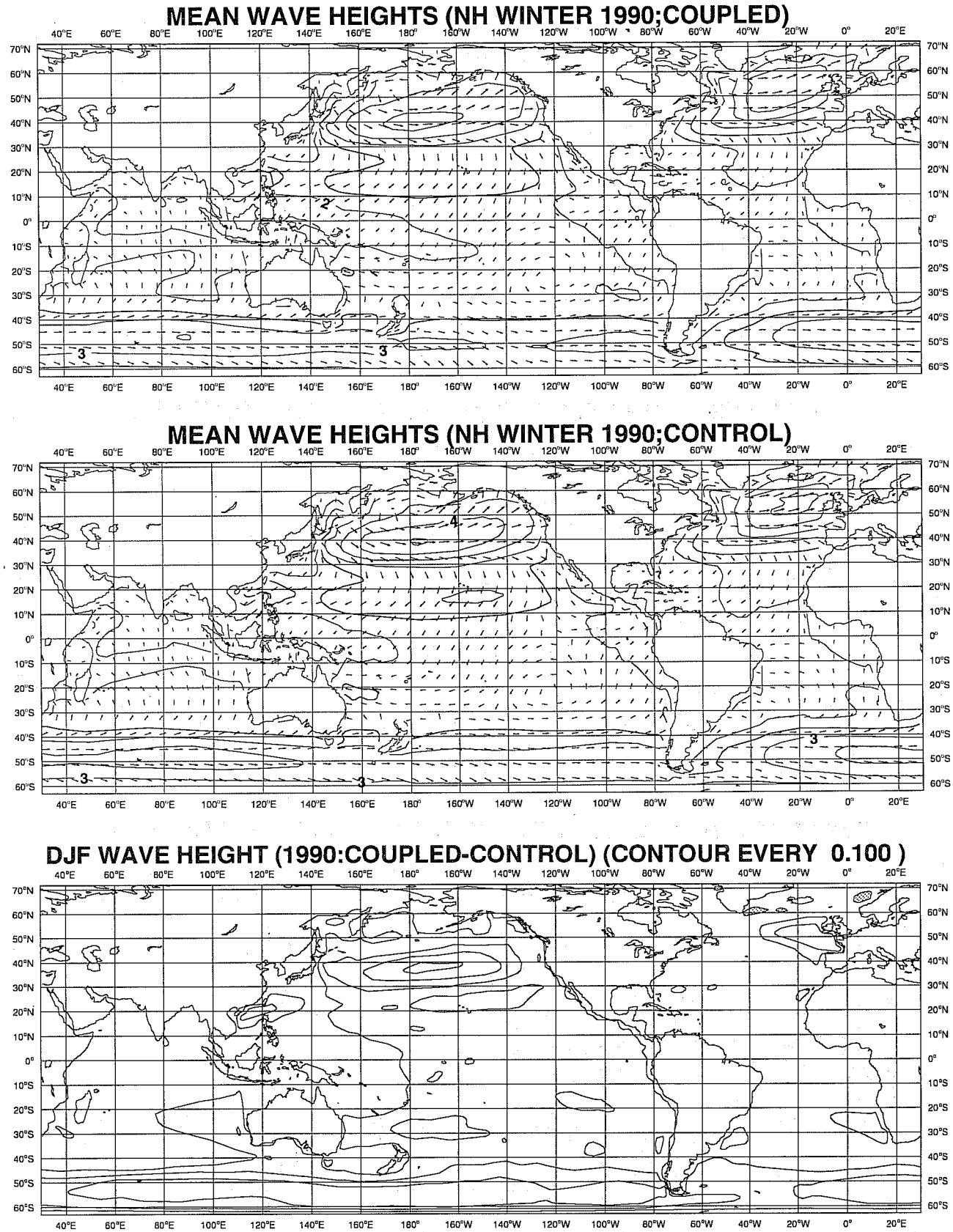

Fig 10 Ensemble mean of wave height for coupled and control run and their differences.

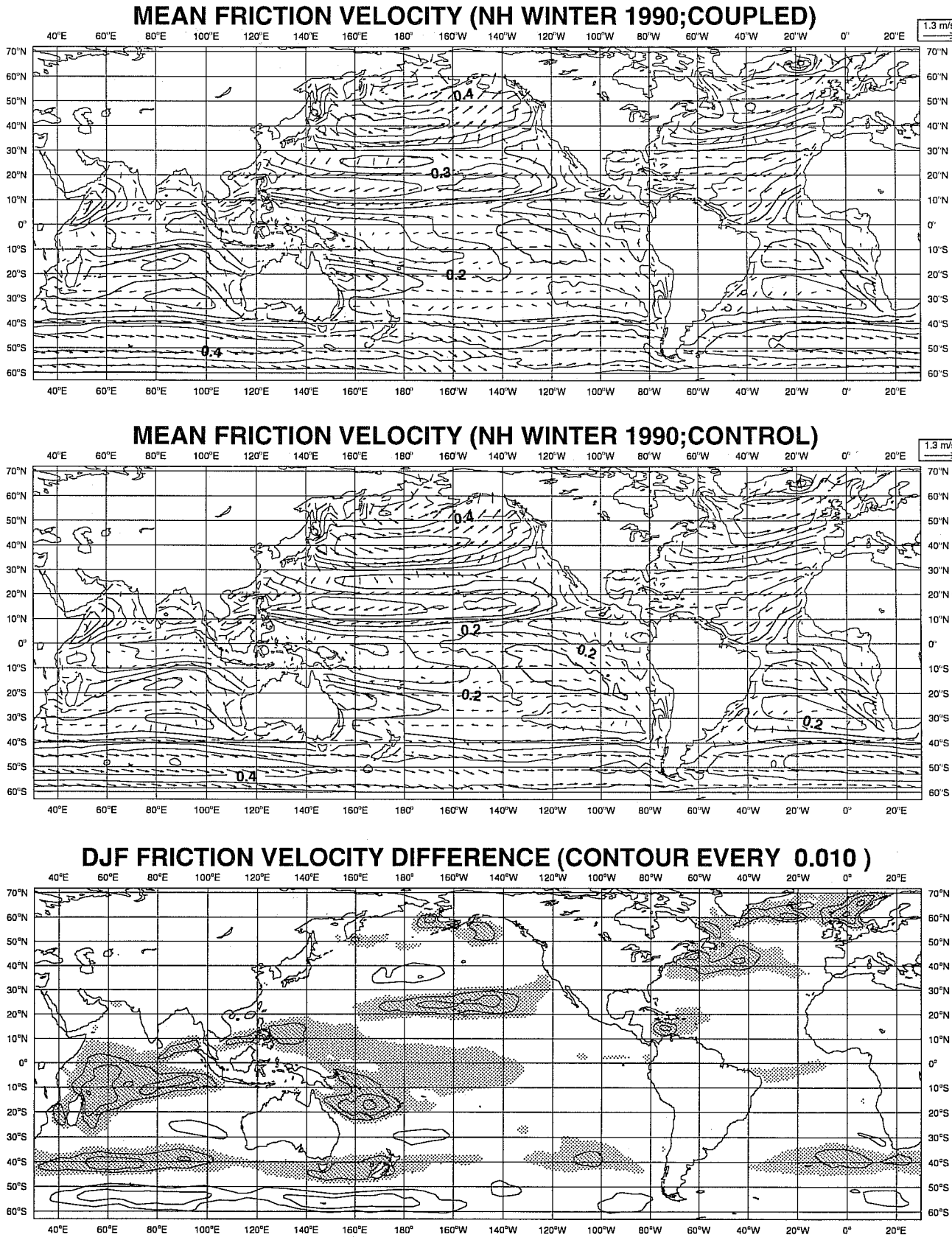

Fig 11 Same as Fig 10 but now for friction velocity. Shading denotes positive differences.

Hence, the atmospheric model was modified in the manner described in the previous Section to allow for two-way interaction while also the analysis suite was changed in order to modify the first-guess in a manner consistent with the coupled physics. Most of the experiments were done with the 3DVAR assimilation system, and in the first-guess step it is then possible to assimilate Altimeter wave height data. Recently, we upgraded our coupled system by using the 4DVAR assimilation scheme; in that event Altimeter data are assimilated in the final trajectory calculation.

Most of the results here were obtained with the T213/L31-1.5D version of the coupled system. The atmospheric model was CY16R2. We performed analyses and forecasts over two periods of 21 days in February 1997 and July 1996. Altimeter data were not used in the analysis, so they may give an independent check on the quality of the wave height field. The next step was to upgrade the coupled system by increasing the wave model resolution from 1.5 deg to 0.5 degree and to allow for the assimilation of Altimeter data. Using CY16R3 of the atmospheric model we redid the first 15 days of February 1997. The assimilation scheme was 3DVAR. Finally, we combined the 4DVAR assimilation scheme and the coupled system and as a technical check we did 10 days of analyses and forecasts over a period in December 1997. We will discuss the quality of the coupled analysis using the first set of experiments. The forecast performance of the coupled system is illustrated by two synoptic examples while we also present a selection of scores for atmospheric and wave parameters.

4.1 Analysis differences

By inspecting synoptic charts we compared the differences in analysed 1000 mb geopotential height from the coupled and control run. In the Northern Hemisphere we found differences in surface pressure of at most 1 mb while in data void areas such as the Southern Atlantic differences were occasionally more substantial. An example of such a difference is shown in Fig. 12 where we have plotted control (top left panel), coupled (top right panel), operational analysis (bottom right panel) and the difference between coupled and control (bottom left panel) at midnight of the 21rst of February 1997. In terms of surface pressure differences may be as much as 6 mb or occasionally even larger and the question is which analysis is closer to some measure of the truth. Based on the comparison between modelled and Altimeter wave height 12 hours later (not shown), it seems that the coupled analysis is closer to the truth, because the extrema in the coupled analysis are higher (since the analysed low is deeper) and hence there is a better agreement with the observations from the Altimeter.From the statistical comparison between Altimeter wave height and modelled wave height there is however no significant difference between coupled and control. Also, the comparison of first-guess winds with scatterometer winds shows no significant differences.

4.2 Forecast Differences

We first present some synoptic charts to get an idea of the impact of ocean waves on the surface pressure fields. This is then followed by a discussion of scores.

Before we give some examples of differences in the surface pressure field between coupled and control experiments it should be pointed out that it is not possible to give a definite answer to the question what the impact of two-way interaction on the fate of an atmospheric low is. The increased surface roughness caused by young ocean waves could give rise to a stronger cross-isobar flow which would result in an enhanced filling up of lows. On the other hand, the increased roughness may increase the sensible and latent heat flux which may deepen a low because of vortex stretching. In addition, the coupling between wind and waves affects the first guess fields in the assimilation cycle, and it is not clear whether this change in initial condition would deepen or fill a low. However, compared to the 'randomly' selected forecasts that use the same initial condition, the data assimilation experiments have differences between coupled and control that are typically larger by a factor of two.

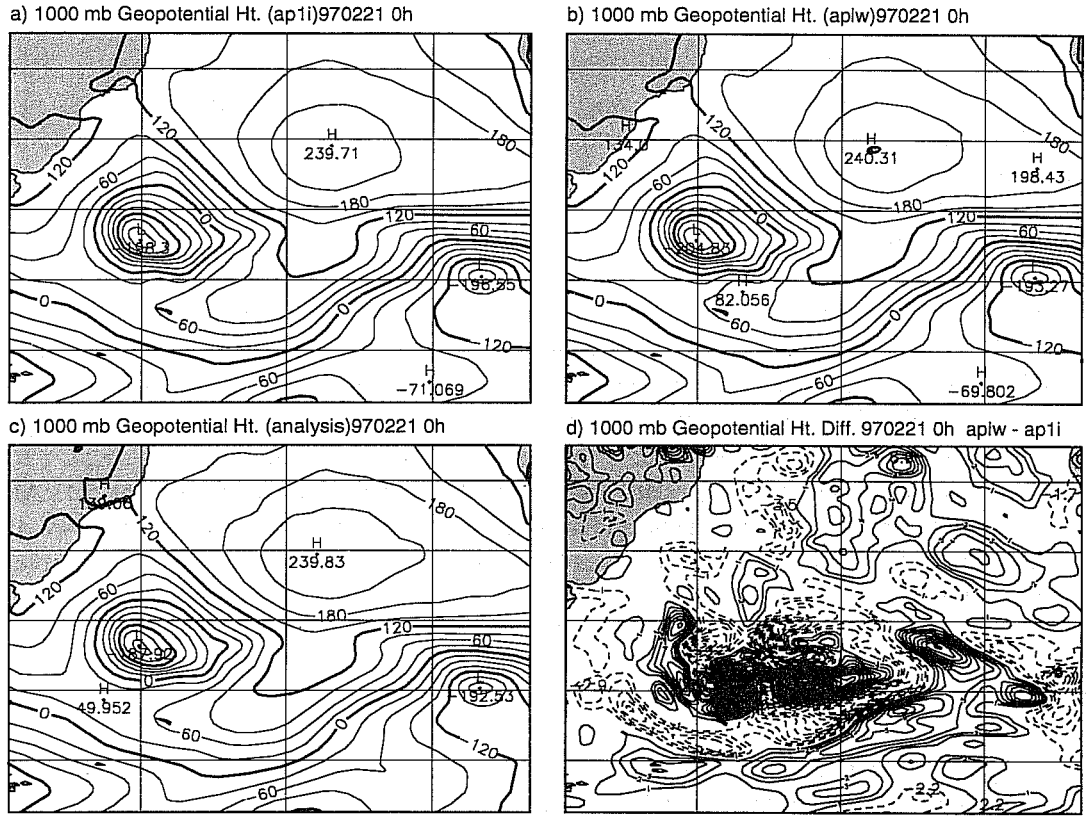

Fig 12 Comparison of analysed 1000 mb geopotential height from control (top left panel), coupled (top right panel), operational analysis (bottom left panel) and the difference between coupled and control (bottom right panel). Area is the Southern Atlantic and the date is midnight, 21st of February 1997.

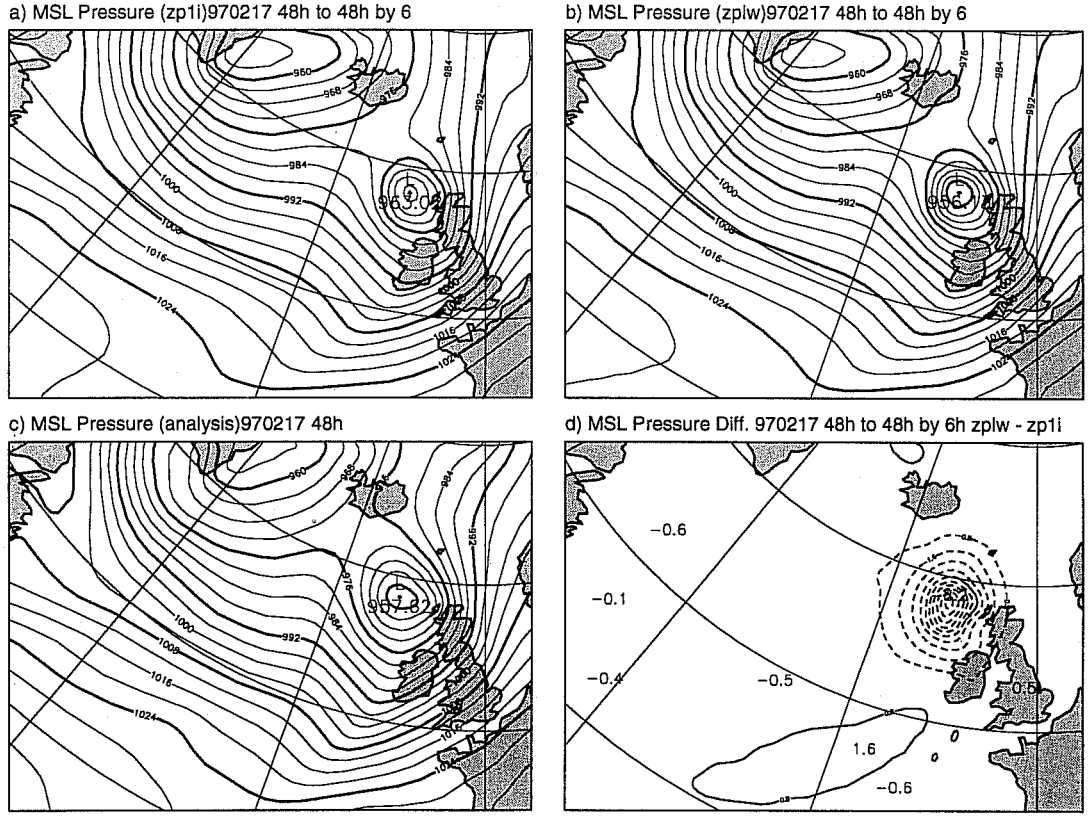

Fig 13 Comparison of 2 day forecast of the FASTEX IOP-17 event from control (top left panel) and coupled (top right panel) experiment. Differences between coupled and control are shown in the bottom right panel while the verifying analysis is from the coupled experiment. Date is the 17th of February 1997.

As a first synoptic example we discuss the impact of the sea state dependent roughness on the rapidly moving low from FASTEX which was discussed already in Section 3. This event started just south of New Foundland and arrived two days later west of Scotland. The day 2 forecast of this case is shown in Fig. 13 and the surface pressure in the coupled run is lower by 7 mb, in good agreement with the coupled analysed pressure of that low (and also with the control analysis, not shown). Such differences in surface pressure result in considerable differences in the strength of the surface wind and therefore also in wave height. In this case the wave height increased from 9 to 13m (not shown). Because of the small scale of the differences there is hardly any change in anomaly correlation over the North Atlantic area; in fact, at day 2 both coupled and control experiment have anomaly correlations close to 100%.

The next example concerns the day 2 forecast of the 24th of December 1997 for the North Pacific and is discussed here because it is an example of large scale impact of two-way interaction on the atmospheric circulation. In this case the resolution of the wave model was 0.5 deg. while the analysis was performed with 4DVAR. The control was provided by the operational run(CY18R3), while the coupled results were obtained from CY18R3 by switching on two-way interaction. Fig. 14 shows the comparison of the coupled day 2 forecast with the control forecast and the control analysis. Substantial large scale differences in the surface pressure can be seen, and a better agreement between coupled forecast and analysis is noted. As a result, considerable improvements in the anomaly correlation for surface pressure were obtained for the whole 10 day forecast range as shown in Fig. 15. The different pressure distributions result in differences in wind field and wave height field. Fig. 16 shows the comparison between coupled wave height forecast, control forecast and verifying analysis on midnight of the 27th of December 1997. Differences between coupled and control wave height reach 4 m and the coupled forecast is in better agreement with the verifying analysis, while the control forecast is too high. This finding agrees with our remarks in Section 2 that the control forecasting system systematically has too high waves in particular in the later stages of the forecast range.

It is concluded that under extreme conditions there is impact of two-way interaction on storm systems, and as a consequence of the modified wind fields this affects the wave height fields as well. Normally, the impact on the weather patterns is small scale.

Let us now discuss some of the forecast scores of the experiments we have performed. We remark that the wave scores are quite sensitive to the verifying analysis that is used and therefore we only present wave scores against their own analysis. As a consequence, the number of forecast cases is limited.

As an illustrative example of the impact of two-way interaction on the forecast performance of wave height we show in Fig.17 for the July period in 1996 anomaly correlation, standard deviation of wave height error, systematic error and mean of verifying analysis as function of forecast time. The area is the Southern Hemisphere which from a wave forecasting point of view is the most interesting area in this time of the year. In agreement with our expectations from the extend-range simulations we notice a reduction of the systematic error in the later stages of the forecast while we also observe a reduction in the standard deviation of error and improvements in the anomaly correlation of wave height. This is accompanied by a reduction in standard deviation of surface wind speed error (not shown) and a reduction of the rms error in 1000 mb wind as shown in Fig.18 for the full period in question. The scores of 500 mb geopotential height for Europe and the North Atlantic for this period are given in the Figs 19. Even in the summer time there may be impact of two-way interaction on the atmosphere although there is considerable variability as is evident from the scatter diagram for anomaly correlation for the North Atlantic (not shown).

An example of impact of two-way interaction during the Northern Hemisphere winter is given in Fig.20. The period is 1-15 February 1997 and the model version is T213/L31-0.5D. The area is the North Pacific and there is a modest impact on the scores for 500 mb height to be seen even in the earlier stages of the forecast.

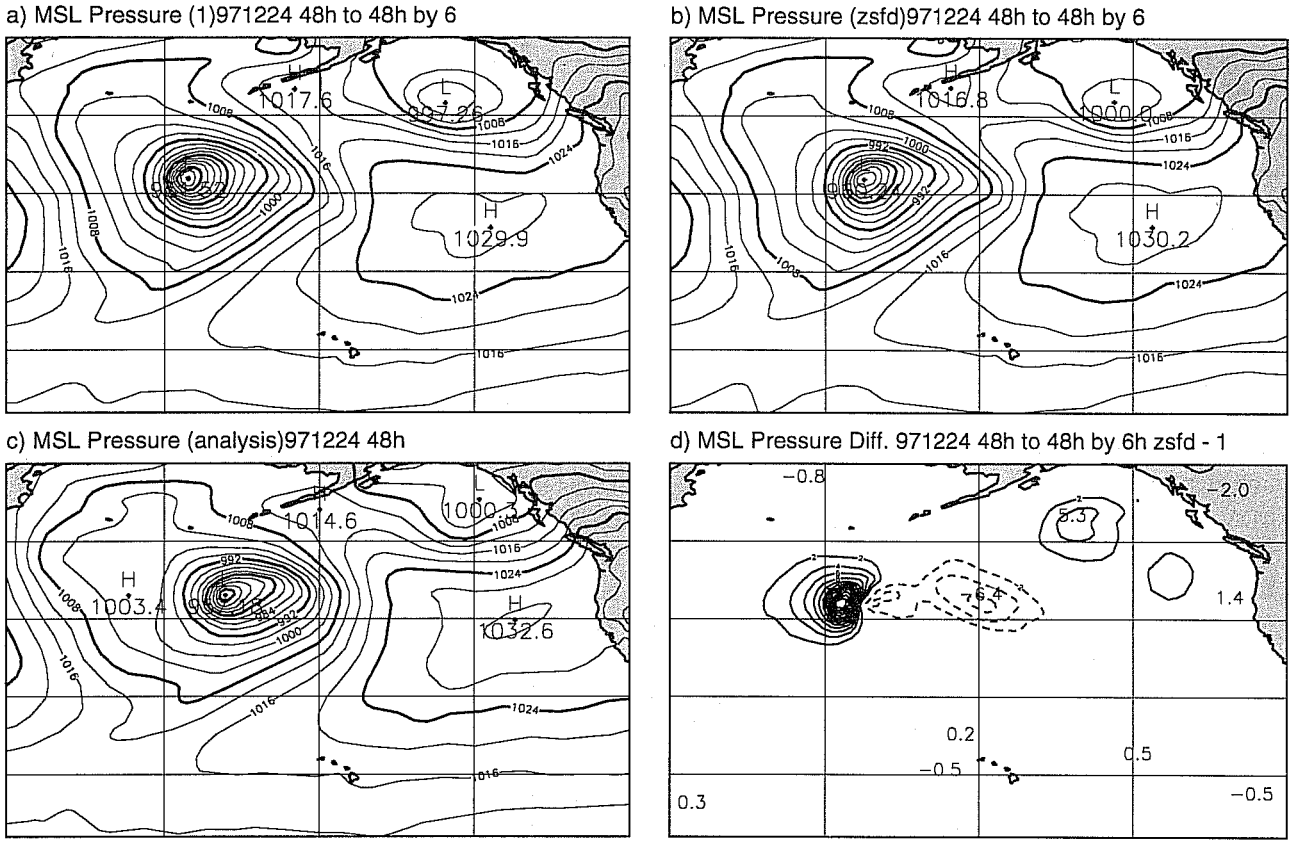

Fig 14 Day 2 forecast of surface pressure for the 24th of December 1997. Area is the the North Pacific.

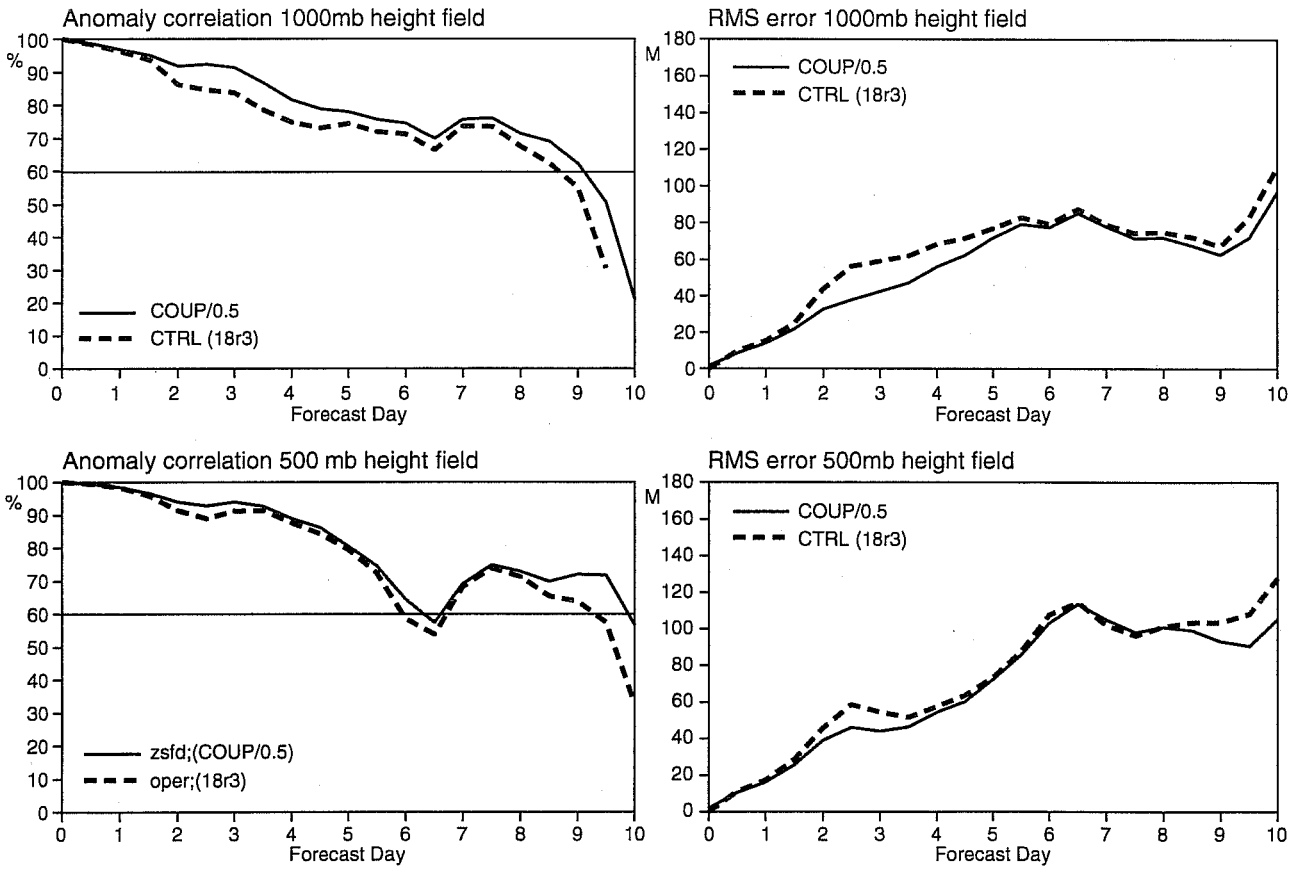

Fig 15 Scores of 1000 and 500 mb height fields for the 24th of December 1997 for the North Pacific.

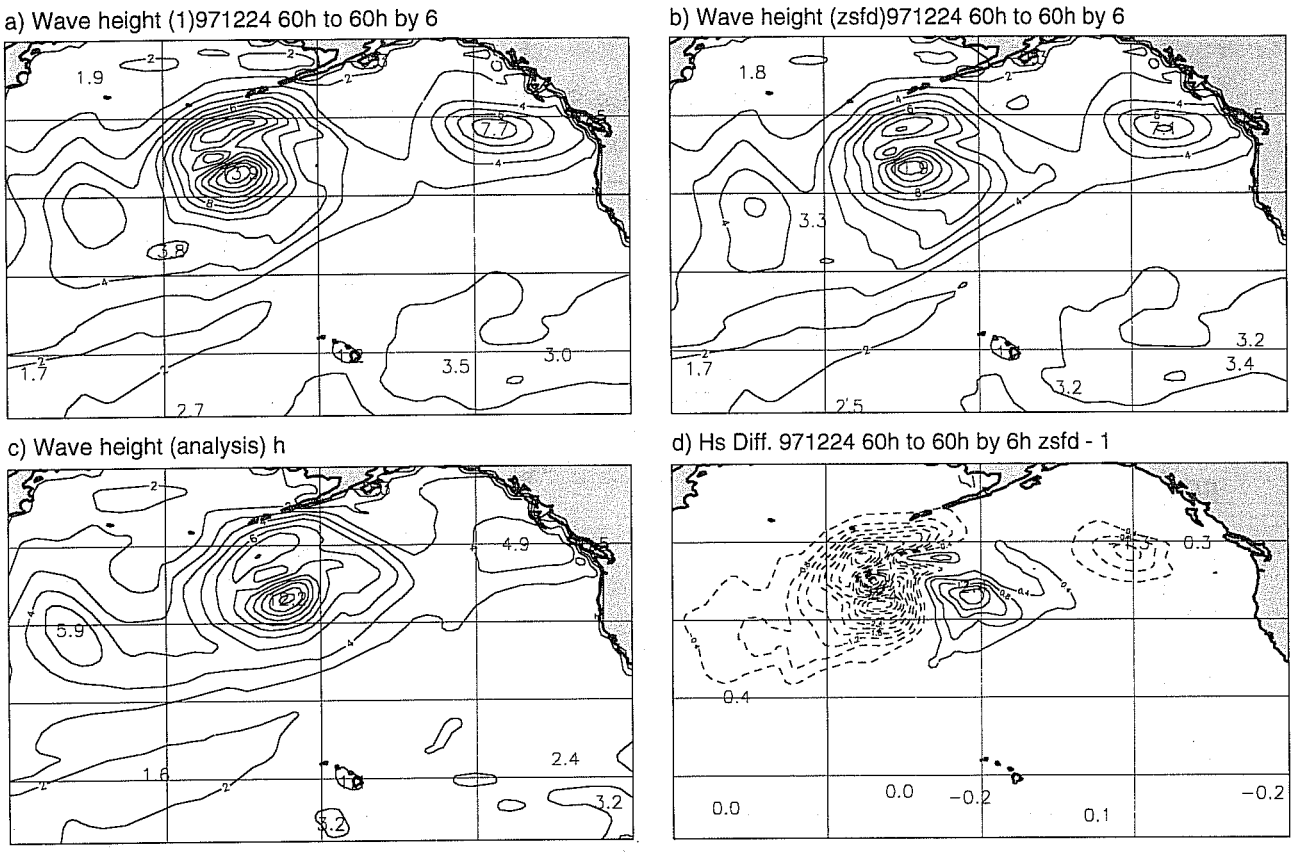

Fig 16 Difference between control (top left panel), coupled (top right panel) and wave height field and the comparison with the operational wave height analysis (bottom left panel).

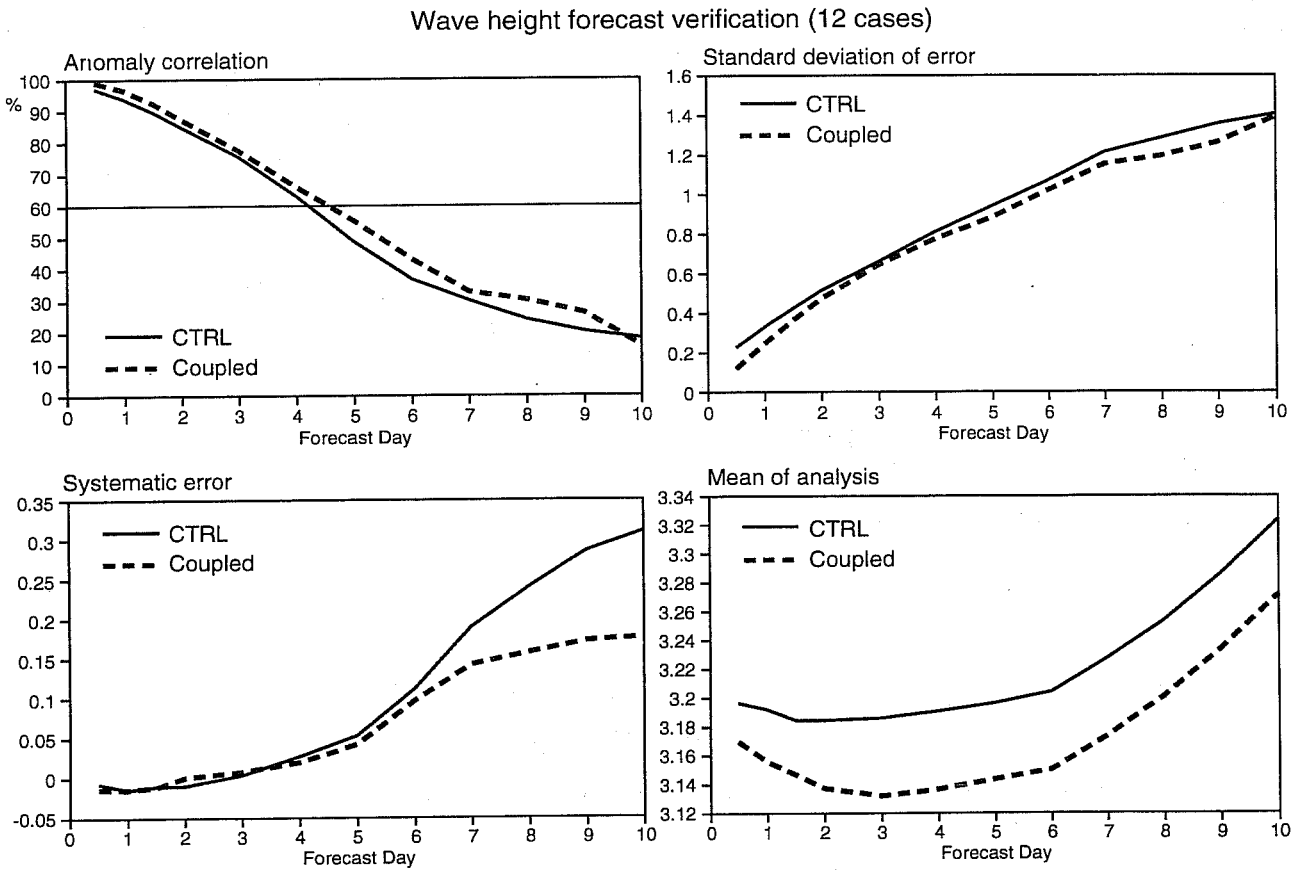

Fig 17 Wave height scores for July period in the southern hemisphere. Verification is against own analysis.

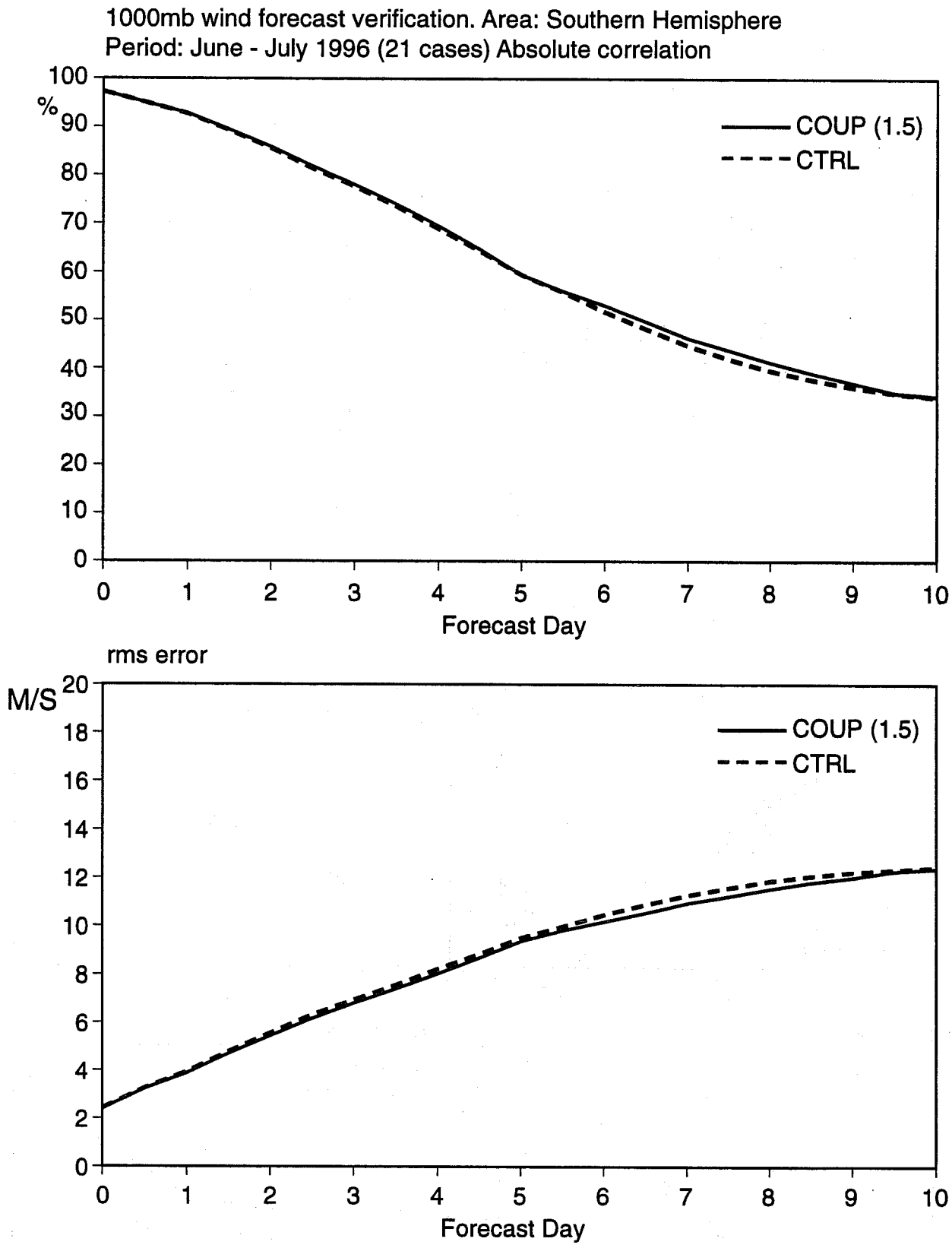

Fig. 18 Rms scores for 1000 mb wind in the Southern Hemisphere for full July period. Verification against operational analysis.

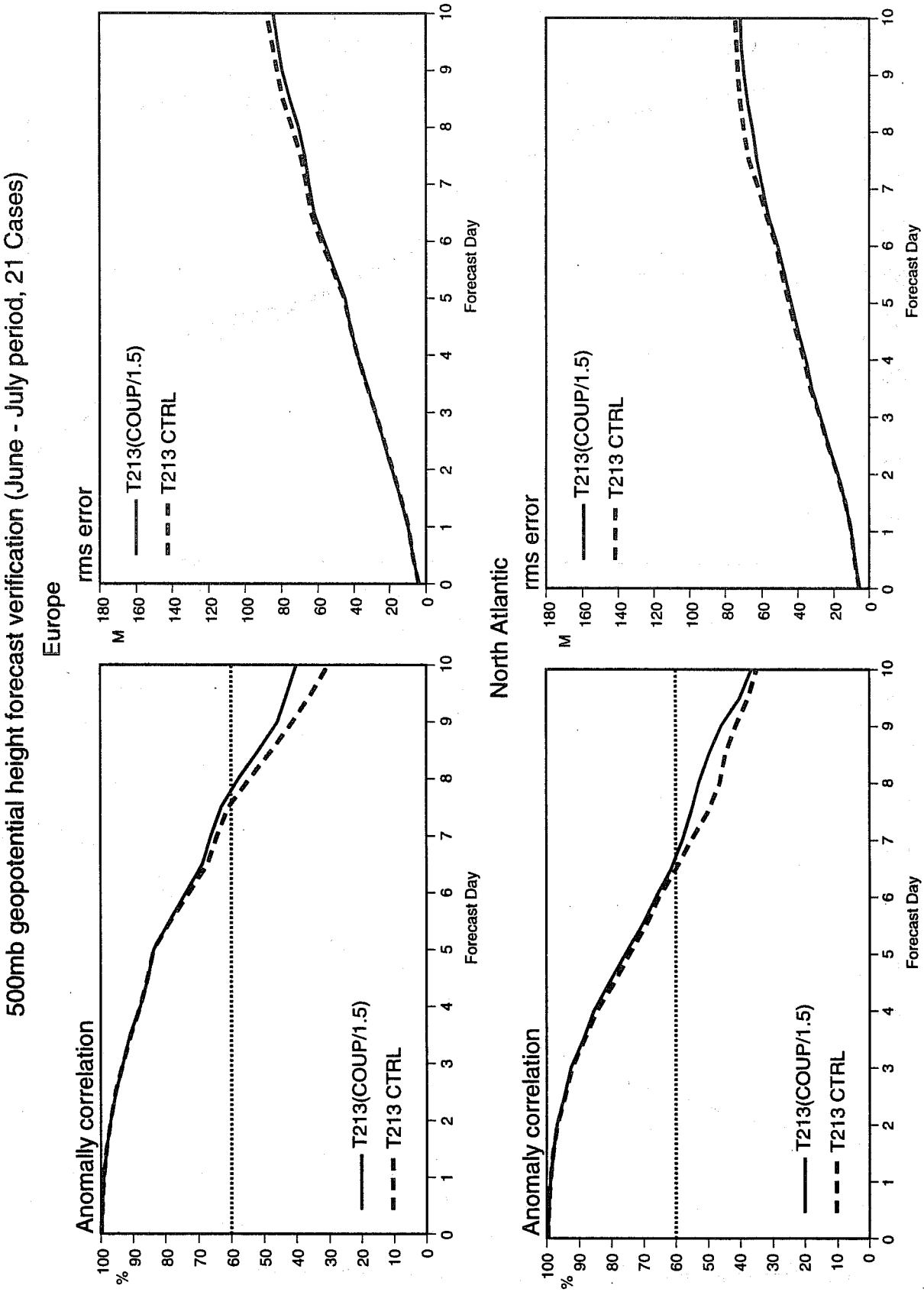

Fig 19 Scores of 500 mb height field for Europe and North Atlantic for the full July period.

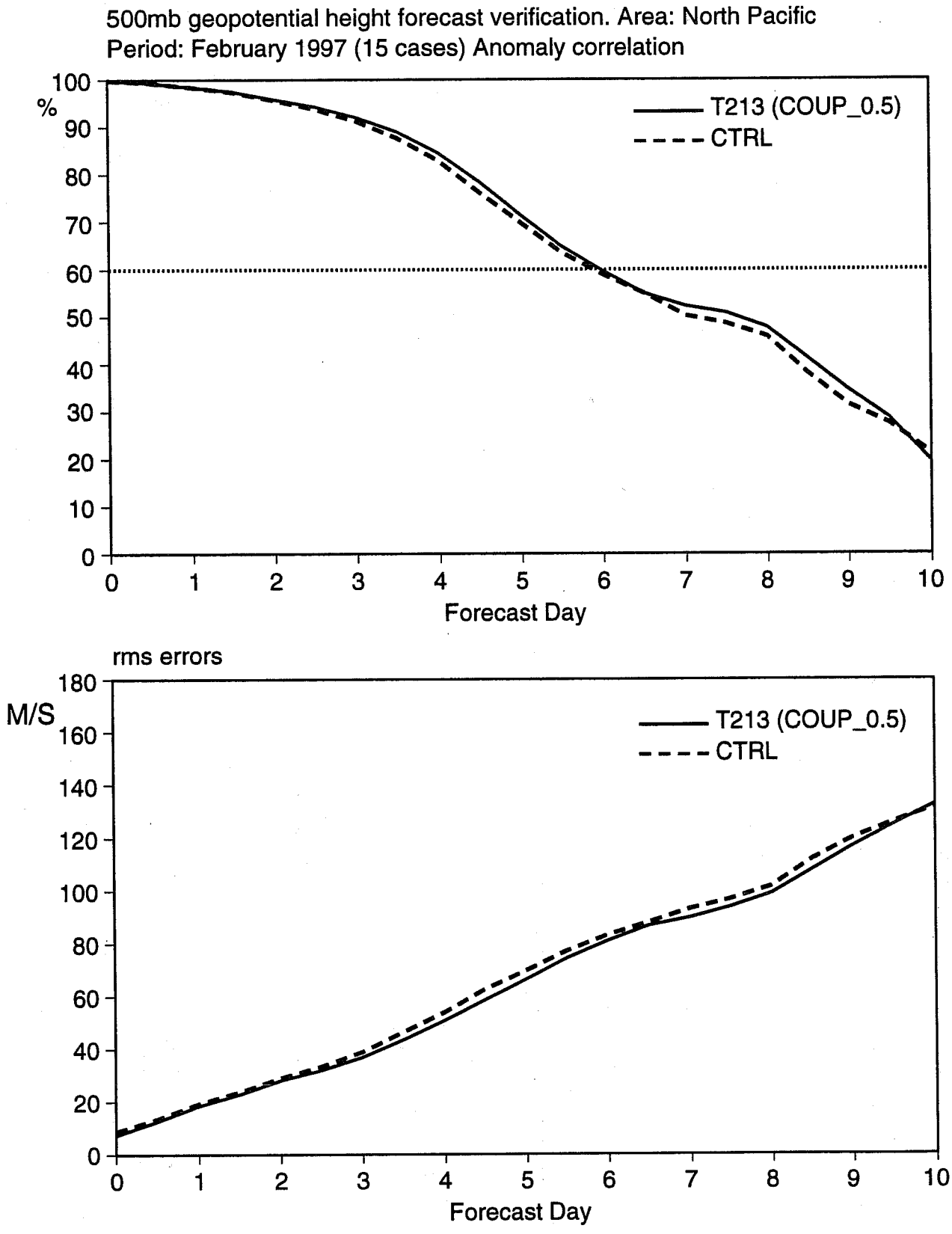

Fig 20 North Pacific scores for 1000 mb height for 15 days in February 1997.

To summarize our findings, it is concluded that although there may be considerable impact of two-way interaction on synoptic cases there is, because of the relatively small scale of the impact, only a modest positive impact on the scores of the atmospheric parameters. Furthermore, another reason for the relatively modest impact on the atmospheric scores may be that extreme events, where one would expect a substantial impact of two-way interaction, occur not very frequently. The impact on the wave height scores seems to be more substantial. A reason for this is that the wave forecast depends to a large extent on the quality of the small scale features in the driving wind field.

5. CONCLUSIONS

Operational experience with wave modelling at many weather institutes indicates that wave forecasts provide a useful tool for marine forecasters. In addition to these practical benefits, it is known that the stand-alone version of the WAM model at ECMWF has provided useful diagnostic information to improve the performance of the atmospheric forecast model, as discussed by *Janssen et al*(1997).

A coupled wind-wave system (with two-way interaction) could provide these advantages together with the following potential benefits:

a) There is evidence that a high resolution (30 km) coupled wind-wave forecast model is sensitive to wave effects (*Doyle*, 1994), but as discussed here this impact seems to depend in a sensitive manner on the resolution of the atmospheric model (and to a lesser extent on the resolution of the wave model).

b) There is evidence that coupling the ocean wave to the ECMWF model has beneficial impact on the systematic errors of the modelled climate in the Northern Hemisphere, and that it may alleviate the wind-speed bias in the medium-range forecasts, especially in the Southern Hemisphere.

c) Furthermore, there is evidence that two-way interaction has a modest positive impact on the medium-range atmospheric forecast, while there is larger impact on the wave height scores.

d) In the context of Ensemble Prediction a coupled wind-wave system has benefits because the ensemble products for waves are then readily available for applications such as ship routing.

e) Finally, the available observational data on waves (from Altimeter and SAR) could provide useful information for atmospheric data assimilation, because of the strong interaction of wind and waves. Four-dimensional variational data assimilation in a coupled system would provide consistent wind and wave fields, with the wave information helping to improve the atmospheric wind and temperature fields through the depth of the troposphere.

Although the results available to date on the benefits of a coupled wind wave assimilation/forecast system are preliminary in nature, they are positively encouraging. Anticipating the development of one model for our geosphere, the ocean waves could provide the necessary interface between the ocean and atmosphere. It is of interest to study in this context the consequences of the modified surface stresses on the tropical ocean circulation and the sea surface temperature distribution. Therefore, it is of interest to study the impact of ocean waves on the results of seasonal forecasts (*Palmer and Anderson*, 1994).

Though *Hasselmann* (1990) could only dream about the advantages of having ocean waves as an interface between the ocean and the atmosphere, it seems that presently the benefits of ocean wave modelling for atmospheric modelling are close to realisation.

REFERENCES

Banner, M L, 1990: Equilibrium spectra of wind waves. J Phys Oceanogr, 20, 966-984.

Beljaars, A C M, 1995: The impact of some aspects of the boundary layer scheme in the ECMWF model, ECMWF seminar proceedings on: Parametrization of Sub-Grid Scale Physical Processes, September 1994, Reading.

Chalikov, D V and V K Makin, 1991: Models of the wave boundary layer. Bound Layer Meteor, 56, 83-99.

Charnock, H, 1955: Wind stress on a water surface. Quart J Roy Meteor Soc, 81, 639-640.

Donelan, M, 1982: The dependence of the aerodynamic drag coefficient on wave parameters. Proc of the First Int Conf on Meteorology and Air-Sea Interaction of the Coastal Zone, The Hague, The Netherlands, American Meteorological Society, 381-387.

Doyle, J D, 1994: Air-sea interaction during marine cyclogenesis. Proc of the Life Cycles of Extratropical Cyclones, Bergen.

Fabrikant, A L, 1976: Quasilinear theory of wind-wave generation. Izv Atmos Ocean Phys, 12, 524-526.

Ferranti, L, F Molteni,? Brankovi? and T N Palmer, 1994: Diagnosis of extratropical variability in seasonal integrations of the ECMWF model. Journal of Climate, 7, 849-868.

Gelci, R, H Cazalé and J Vascal, 1957: Prévision de la Houle. La méthode des densités spectro angulaires. Bull Inform Comité Central Oceanogr d'Etude Côtes, 9, 416-433.

Hasselmann, K, 1960: Grundgleichungen der Seegangsvoraussage. Schiffstechnik, 7, 191-195.

Hasselmann, K, 1990: Waves, dreams and visions, John Hopkins APL Technical Digest, 11, 366-369.

Hasselmann, K et 15 al., 1973: Measurements of wind-wave growth and swell decay during the JOint North Sea WAve Project (JONSWAP). Dtsch Hydrogr Z, Suppl A, 8 (12).

Hasselmann, K, 1985: Assimilation of microwave data in atmospheric and wave models in the use of satellite data in climate models. Proc Conf Alpbach, 47-52 (ESA SP-244).

Hasselmann, S, K Hasselmann, J H Allender and T P Barnett, 1985: Computations and parametrizations of the nonlinear energy transfer in a gravity wave spectrum. Part II. Parametrizations of the nonlinear energy transfer for application in wave models. J Phys Oceanogr, 11, 1373-1391.

Hasselmann, K and S Hasselmann, 1991: On the nonlinear mapping of an ocean wave spectrum into a SAR image spectrum and its inversion. J Geophys Res, C96, 10713-10729.

Janssen, P A E M, 1982: Quasilinear approximation for the spectrum of wind-generated water waves. J Fluid Mech, 117, 493-506.

Janssen, P A E M, 1989: Wave-induced stress and the drag of airflow over sea waves. J Phys Oceanogr, 19, 745-754.

Janssen, P A E M, 1991: Quasilinear theory of wind wave generation applied to wave forecasting. J Phys Oceanogr, 21, 1631-1642.

Janssen, P A E M, 1992: Experimental evidence of the effect of surface waves on the airflow. J Phys Oceanogr, 22, 1600-1604.

Janssen, P A E M, 1994: Results with a coupled wind wave model. ECMWF Technical Report No. 71.

Janssen, P A E M, A C M Beljaars, A Simmons and P Viterbo, 1992: The determination of the surface stress in an atmospheric model. Mon. Wea. Rev, 120, 2977-2985.

Janssen, P A E M and P Viterbo, 1996: Ocean waves and the atmospheric climate. J Climate, 9, 1269-1287.

Janssen, P A E M, B Hansen and J Bidlot, 1997: Verification of the ECMWF Wave Forecasting System against Buoy and Altimeter Data. Weather and Forecasting, 12, 763-784.

Komen, G J, K Hasselmann and S Hasselmann, 1984: On the existence of a fully developed windsea spectrum. J Phys Oceanogr, 14, 1271-1285.

Komen, G J, L Cavaleri, M Donelan, K Hasselmann, S Hasselmann, P A E M Janssen, 1994: Dynamics and modelling of ocean waves. Cambridge University Press.

Lionello, P and P A E M Janssen, 1990: Assimilation of altimeter measurements to update swell spectra in wave models. Proc of the international symposium on assimilation of observations in meteorology and oceanography. Clermont-Ferrand, France, p 241-246.

Lionello, P, H Günther and P A E M Janssen, 1992: Assimilation of altimeter wave data in a global ocean wave model. J Geophys Res, C97, 14453-14474.

Mitsuyasu, H, 1968: On the growth of the spectrum of wind-generated waves. 1. Rep Res Inst. Appl. Mech, Kyushu Univ., 16, 459-465.

Mitsuyasu, H, 1969: On the growth of the spectrum of wind-generated waves. 2. Rep Res Inst. Appl Mech, Kyushu Univ, 17, 235-243.

Palmer, T N and D L T Anderson, 1994: The prospects for seasonal forecasting - a review paper, Q J R Meteorol. Soc, 120, 755-793.

Pedlosky, J, 1987: Geophysical Fluid Dynamics, Springer-Verlag, New York.

Phillips, O M, 1958: The equilibrium range in the spectrum of wind-generated ocean waves. J FLuid Mech, 4, 426-434.

Smith, S D, R J Anderson, W A Oost, C Kraan, N Maat, J De Cosmo, K B Katsaros, K Davidson, K Bumke, L Hasse, H M Chadwick, 1992: Sea surface wind stress and drag coefficients: The HEXOS RESULTS. Bound-Layer Meteor, 60, 109-142.

Stoffelen, A and D Anderson, 1995: The ECMWF contribution to the characterisation, interpretation, calibration and validation of ERS-1 scatterometer backscatter measurements and winds and their use in numerical weather prediction models. ECMWF Technical Report.

Weber, S, H von Storch, P Viterbo and L Zambresky, 1993: Coupling an ocean wave model to an atmospheric general circulation model. Climate Dynamics, 9, 63-69.